SAND76-0165
Unlimited Release

NRC-7

Annular Core Pulse Reactor Upgrade Quarterly Report October - December 1975

Reactor Research and Development Department

Prepared by Sandia Laboratories, Albuquerque, New Mexico 87115 and Livermore, California 94500 for the United States Nuclear Regulatory Commission under ERDA Contract AT(29-1)-789.

Printed April 1976

Sandia Laboratories

SF 2900 Q(7-73)

Nuclear Fuel Cycle Programs

Issued by Sandia Laboratories, operated for the United States
Energy Research and Development Administration by Sandia Corporation

SAND76-0165
Unlimited Release
Printed April 1976

NRC-7

ANNULAR CORE PULSE REACTOR UPGRADE QUARTERLY REPORT*
October - December 1975

Submitted by

Reactor Research and Development Department
Sandia Laboratories, Albuquerque, New Mexico 87115

APPROVED: ______________________
Manager, Reactor Research and Development

____
Director, Nuclear Fuel Cycle Programs

*This work was supported by the U. S. Nuclear Regulatory Commission (Project No. A1032) and the U. S. Energy Research and Development Administration Under Contract AT (29-1)-789.

CONTENTS

FIGURES

ANNULAR CORE PULSE REACTOR UPGRADE QUARTERLY REPORT

Introduction

During FY75, Sandia Laboratories conducted an Experimental Fast Reactor Safety Research program funded by the Nuclear Regulatory Commission/Division of Reactor Safety Research. A portion of this program involved a feasibility study for performance improvement of the Annular Core Pulse Reactor (ACPR Upgrade). The progress on the ACPR Upgrade during FY75 is described in References 1, 2, and 3. Beginning with FY76, the ACPR Upgrade progress is reported in a quarterly report separate from the report on the Experimental Fast Reactor Safety Research program; this report is described in Reference 4.

Funding for the ACPR Upgrade is being provided jointly by NRC/DRSR and ERDA/DMA since the improved reactor will be beneficial to the programs of both agencies.

The object of the ACPR Upgrade is to arrive at a reactor modification which will provide an increased pulsed neutron fluence in the irradiation cavity without increasing the pulse duration. The upgraded reactor will also have an increased steady-state neutron flux. The approach to the upgrade modification involves a two-region core concept. The inner region, surrounding the irradiation cavity, consists of a high-heat capacity fuel which will sustain a large fission energy deposition. The outer region consists of a uranium-zirconium hydride fuel similar to the present ACPR fuel. This reactor modification will make use of the majority of the existing reactor structure and can be accomplished in a relatively short time.

The ACPR Upgrade project is divided into nine tasks to improve management of the overall project and to maintain close control of the project budget. This report discusses the progress on each task in a separate chapter. The individual tasks and a brief description of each are given below. Major emphasis this quarter has been on fuel material development, fuel element design, and control system design.

<u>Task 1. Safety, Documentation, and Compliance</u> (J. A. Reuscher, Supervisor)

This task involves the preparation of the safety analysis report and the technical specifications for the upgraded reactor. These documents must be submitted to ERDA/DOS for review and approval prior to startup of the reactor. Compliance with the requirements contained in 10CFR50 is a part of this task; these include an independent design review and quality assurance program. In addition, the initial test planning for the reactor is a part of this task.

Task 2. Core Nuclear Design (R. L. Coats, Supervisor)

This task includes core neutron physics studies, determination of control rod configurations, and the prediction of experimental conditions. Correlation of calculational techniques with the present ACPR is included.

Task 3. Console Development (J. E. Powell, Supervisor)

This task is concerned with the design, development, and procurement of a control system which follows IEEE 279 standards.

Task 4. Mechanical Design (G. W. Barr, Supervisor)

Mechanical design activities for the project include the cooling system, the containment structure, drive mechanisms for the control and transient rods, and the control rod design.

Task 5. Fuel Element Design (J. A. Reuscher, Supervisor)

This task interfaces with the fuel material development tasks (Tasks 6 and 7) and includes the stress analysis and heat transfer studies for design of the high-heat capacity fuel elements. The fuel element demonstration tests are also a part of this task.

Task 6. Primary Fuel Material Studies (R. L. Coats, Supervisor)

The primary fuel material (at the present time) is $BeO\text{-}UO_2$ since it offers the largest performance improvement for the upgrade. This task involves the development of fabrication techniques, material compatibility studies, material property determinations, material analysis, and in-pile experiments for pulse testing of fuel geometries.

Task 7. Secondary Fuel Material Studies (C. H. Karnes, Supervisor)

The secondary fuel material is (UC-ZrC)-graphite which will be used in the high-heat capacity fuel element if the $BeO\text{-}UO_2$ does not prove feasible. This task involves the development of fabrication techniques, material compatibility studies, material property determinations, material analyses, and in-pile experiments.

Task 8. Driver Core Fuel Element (J. A. Reuscher, Supervisor)

The testing of the outer core fuel material and the design of the driver core fuel element are the objectives of this task. This fuel is a uranium-zirconium hydride which is similar to the present ACPR fuel. The hydrogen-to-zirconium ratio is decreased slightly for the upgraded reactor. The testing of this fuel includes pellet tests and prototype element tests.

Task 9. Diagnostic System (J. E. Powell, Supervisor)

This task involves the development of a fuel motion detection system for fissile experiments in the upgraded ACPR. Such a system allows the detection of molten fuel motion in a reactor experiment. Several schemes are under development and involve both in-core and out-of-core devices. Progress on this task is reported as part of Sandia's Fast Reactor Safety Research Program (Ref. 5).

Project Schedule

The schedule for the ACPR Upgrade is shown in Figure 1. This figure gives the major events in the project and projects an operational date (critical experiment) about January 1978. This schedule is based upon release of project funds in January 1976. A detailed PERT analysis of the overall project has been conducted and the critical paths have been identified. The PERT chart is too detailed to include in this report.

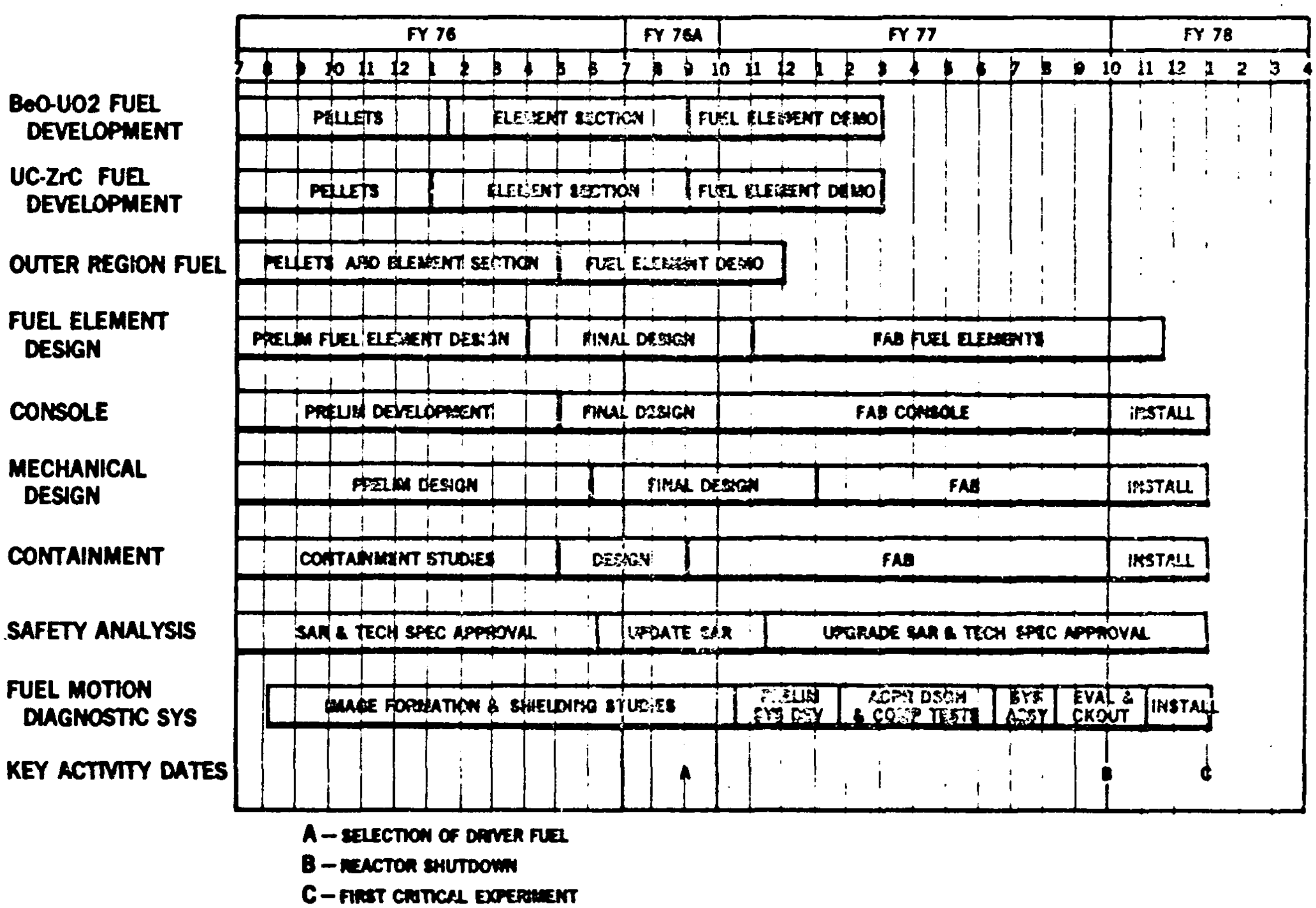

Figure 1. ACPR Upgrade Schedule

CHAPTER I

TASK 1. SAFETY, COMPLIANCE, AND DOCUMENTATION

J. A. Reuscher, 5421; B. F. Estes, 5421

Introduction

This task involves the preparation of the safety documentation for the ACPR Upgrade and compliance with ERDA regulations concerning reactor design and construction.

Safety Analysis Report (SAR)

The revised draft Safety Analysis Report for the present ACPR completed its review and publication process during this quarter. This document follows the format and structure required by the Nuclear Regulatory Commission for safety analysis reports of power reactors. The revised draft ACPR SAR has a length of approximately 1200 pages and required a manpower effort of about four man years. This draft document will be modified to reflect the changes in the reactor systems for the ACPR Upgrade. Data and computations to be used in the modified version are reported throughout this document.

CHAPTER II

TASK 2. CORE NUCLEAR DESIGN

P. S. Pickard, 5422; D. J. Sasmor, 5422

Introduction

Neutronics studies were performed for several aspects of the ACPR upgraded core design during this past quarter. The majority of these studies were intended to provide additional details and perspectives in areas of core design which had been examined previously in survey calculations. Detailed calculations using one-dimensional S_N analysis were performed to examine performance, criticality, and fuel temperatures for all upgrade configurations for the UO_2-BeO and UC-ZrC-C fuel candidates. Two-dimensional S_N calculations were performed to verify the 1-D results. These calculations are being compiled and summarized for the UO_2-BeO fuel candidate.

The summary of important parameters has focused initially on fluence, criticality, and fuel temperature and stress. The summary calculations evaluated a given core design approach by determining the fluence attainable for a peak hydride temperature of 1000° C, the effective multiplication constant, and the approximate temperature drop across the radius of the fuel pellet and maximum fuel temperature.

Calculations For BeO-UO_2 Central Region

A series of these calculations for a range of hydride and high-heat capacity fuel loading allows the construction of a plot of pulse performance with a family of criticality and maximum fuel temperature constraint curves. An example of this approach for the UO_2-BeO core design calculations is shown in Fig. 2. The pulse fluence improvement is plotted versus fuel loading in the high heat capacity fuel. Interpolation between the criticality and temperature constraints allows the determination of the optimum configuration for a given eigenvalue and stress level. The core configuration of Fig. 2 consisted of three inner rows of UO_2-BeO and niobium liners and three outer rows of U-$ZrH_{1.5}$. Normal operation with this configuration requires a calculated eigenvalue of 1.07 to 1.08 with large negative experiments or a core slot requiring eigenvalues of 1.09 to 1.12. The performance figures shown

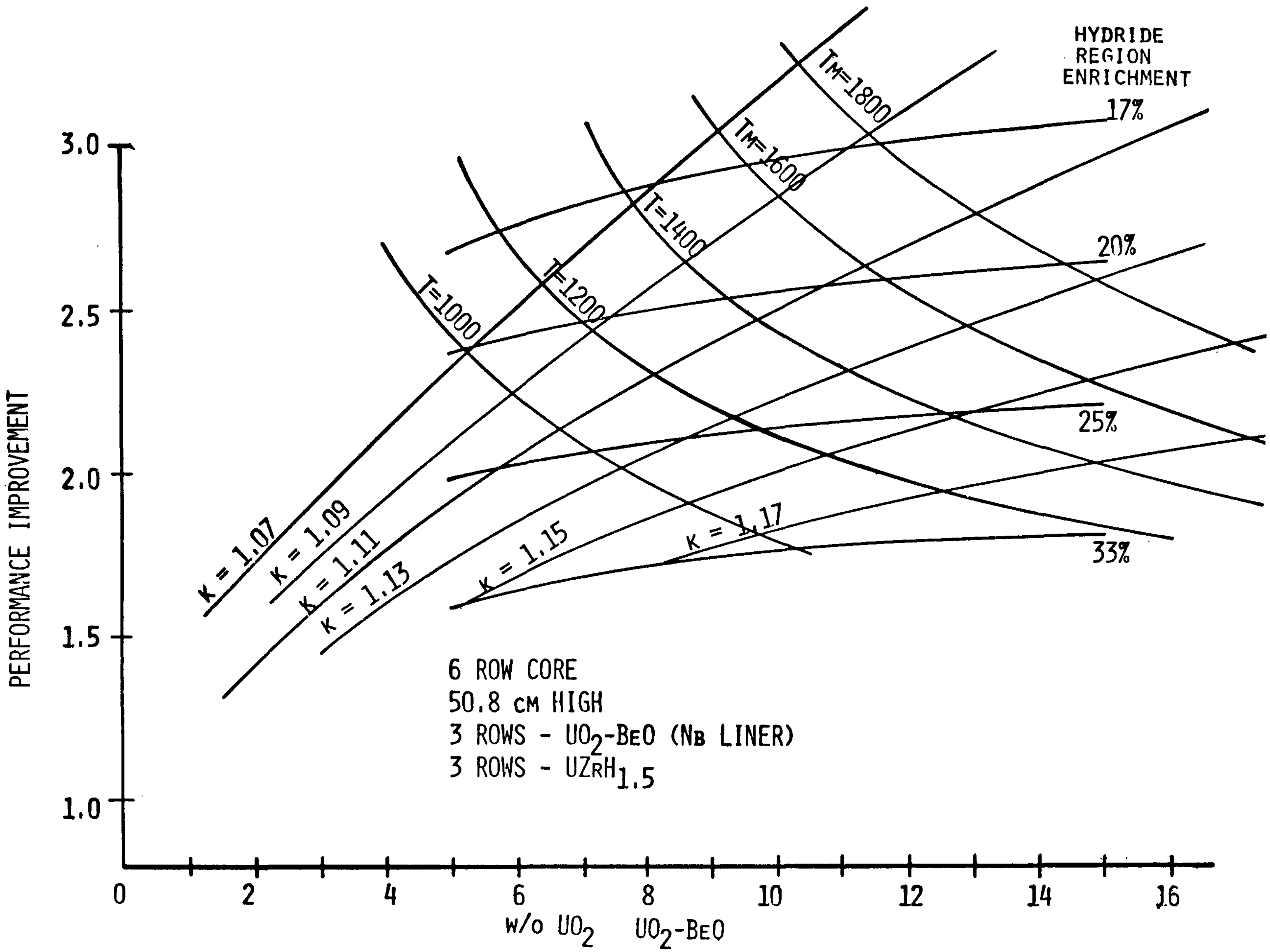

Figure 2. Performance Improvement in UO_2-BeO, U-$ZrH_{1.5}$ Two-Region Core Based on 1000^{o} C Rise in Hydride Fuel Temperature

apply to an unperturbed core. Performance degradation with a core slot of two rows of fuel is estimated to be approximately 20 percent. The permissible temperature and stress levels for the dual annuli fuel pellet design have not been established in in-pile multiple pulse tests for the UO_2-BeO fuel material. Single pulse tests performed to date suggest that 1000° to 1200° C may be attainable in the upgraded core. At these levels the anticipated performance improvement factor for the unperturbed core is approximately 2.35 to 2.55. Additional fuel test results are required to determine final core configuration and performance.

Figure 2 is an example of the initial calculations, and further calculations are required to provide the same display of design information for the modifications in core design directed toward temperature and stress reduction. The core design modifications being analyzed include reduced loading elements in interface rows, clad and liner material changes, effects of core size changes, and reflector element studies.

Calculations for (UC-ZrC)-Graphite Central Region

A comparative set of performance criticality-temperature curves are shown in Fig. 3 for the UC-ZrC-C fuel candidate. These calculations utilized one-dimensional transport analysis with AMPX-derived, 9-energy group cross sections. The UC-ZrC-C fuel forming the inner region was 30 volume percent UC-ZrC-C, 60 volume percent graphite, and 10 volume percent void. The core configuration consisted of three inner rows of UC-ZrC-C and three outer rows of U-$ZrH_{1.5}$ with a fuel height of 50.8 cm. Assuming fuel temperatures in the range of 2000° to 2300° C are attainable in the graphite lined element, the anticipated performance improvement in the UC-ZrC-C core is 2.2 to 2.4 The lower neutronic worth of the UC-ZrC-C fuel requires increased U^{235} content for a given eigenvalue. Ultimate operational capability of the UC-ZrC-C fuel candidate is anticipated to be determined by fuel element heat transfer considerations.

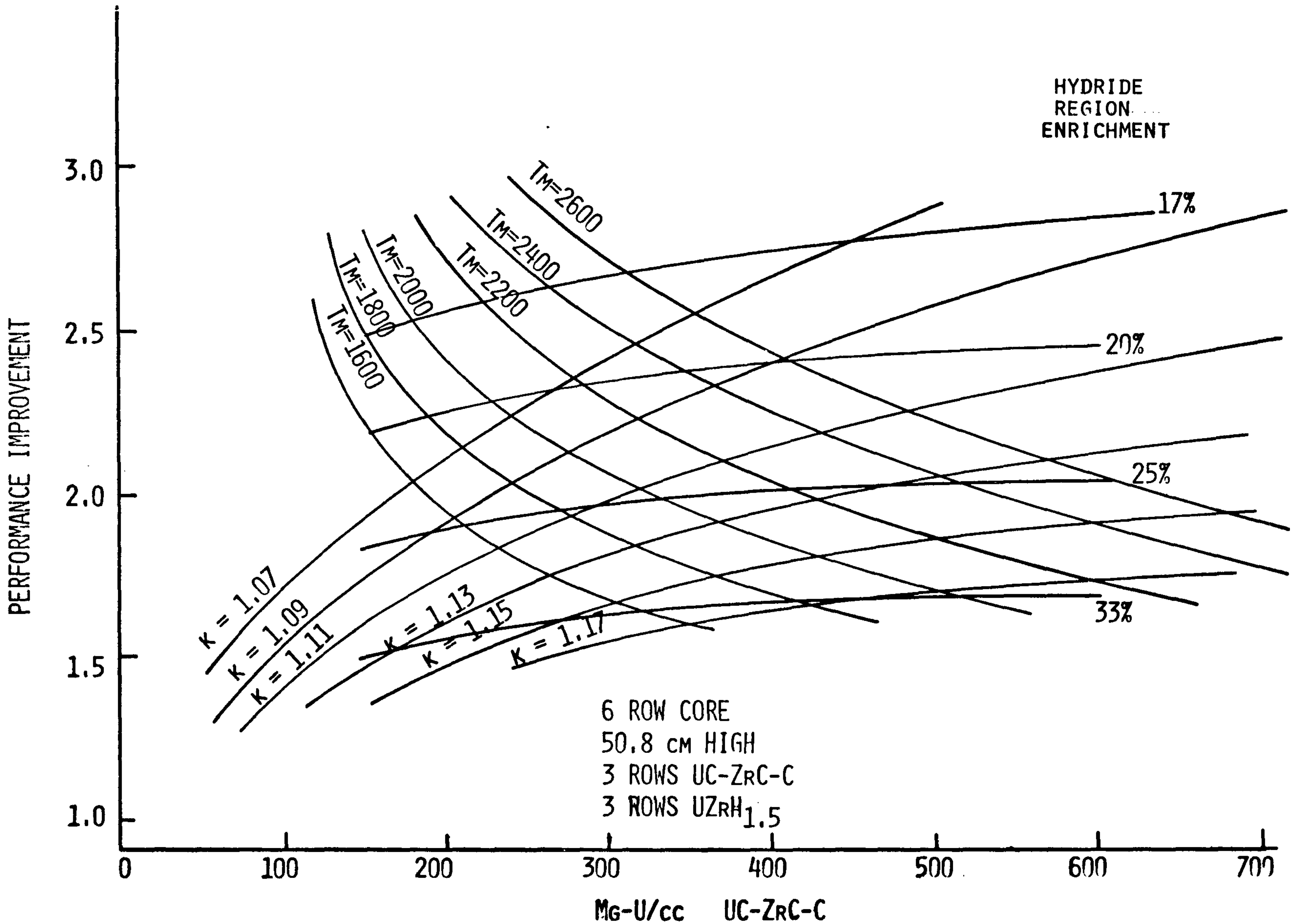

Figure 3. Performance Improvement in UC-ZrC-C, U-$ZrH_{1.5}$ Two-Region Core Based on 1000° C Rise in Hydride Fuel Temperature

CHAPTER III

TASK 3. CONSOLE DEVELOPMENT

W. L. Sullivan, 5423

A block diagram of the control and protect systems has been generated and reviewed with ACPR operations personnel. The required interlock and operating sequence functions have been identified and a truth table of these functions has been generated. These two items essentially complete the basic system definition; however, they will be reviewed and revised at least one more time. This revision should be completed by the end of January, 1976, at which time the detailed system design can begin.

The Gulf Electronic Systems Division was also visited during this quarter to assess their potential as a possible source for the ACPR control and protect systems. Documents describing General Atomic's quality assurance procedures and performance on the Nuclear Safety Research Reactor (NSRR) were obtained. A copy of the IEA-RPZ reactor specifications was also obtained during this visit. As a result of the discussions and a review of the documentation, the following general conclusions were reached:

1. The NSRR system doesn't meet our needs.
2. General Atomic's quality assurance procedures seem to be relatively well documented.
3. The generation of an adequate set of specifications will be more difficult than previously anticipated.
4. General Atomic's technical documentation of the NSRR system is inadequate.

Given a rigorous set of specifications, General Atomic appears to be a viable supplier and, therefore, effort has been directed toward defining the form and content of a satisfactory set of specifications.

CHAPTER IV

TASK 4. MECHANICAL DESIGN

D. K. Overmier, 1134

Containment Studies

A containment scheme which seals the entire ACPR room would seem to be prohibitively expensive, while the use of a walk-in bubble over the reactor could be a major nuisance to operators and experimenters. From the standpoint of economy in construction and convenience of operation, the most promising suggestion for containment would involve a sealed enclosure over the pool in conjunction with a new bridge (or bridges) holding a sealed rod-actuating assembly. This pool closure scheme would serve to contain fission products from a core accident. Containment of experiments would be provided separately.

Cooling System

As yet no design work has been performed. Design data are being assembled to provide a 2 MW cooling capability for the pool water.

Section Test Apparatus

A design for the section test cannister has been completed. The apparatus utilizes a short length of dimpled clad with fittings for temperature and pressure transducers. A purchase requisition for two cannisters has been initiated.

Fuel Element Demonstration Apparatus

The design of the water circulation system for the fuel element demonstration tests has been completed. This apparatus will fit in the ACPR cavity and will be used to provide cooling of the experimental elements under conditions which simulate the upgraded core.

CHAPTER V

TASK 5. FUEL ELEMENT DESIGN

J. A. Reuscher, 5421; C. B. Sisson, 1283

Introduction

This task involves the design and procurement of the high-heat capacity fuel elements for the central region of the core. The results of the in-pile experiment in the fuel material development tasks will be used to define the fuel material and the fuel region configuration. Further reactor tests will examine material compatibility effects, heat transfer characteristics, and safety aspects for various fuel element designs. The major activities for this quarter involved heat transfer calculations for a dual annulus, (UC-ZrC)-graphite, fuel element.

Thermal Model

The fuel element model for the dual annulus, (UC-ZrC)-graphite design was described in detail in the previous quarterly report.[4] The dual fuel annuli are positioned by a central graphite rod with a diameter of 0.64 cm. There is a 0.013 cm gap between the rod and the inner fuel annulus, which has an inner radius of 0.33 cm and an outer radius of 0.98 cm. There is a gap of 0.038 cm between the two fuel annuli, and the outer annulus has an inside radius of 1.02 cm and an outer radius of 1.66 cm. A graphite sleeve acts as a thermal radiation barrier between the fuel and the stainless steel clad. The sleeve is 0.089 cm thick and there is a 0.032 cm gap between the sleeve and the fuel and a 0.038 cm gap between the sleeve and the clad (0.051 cm thick). The clad is surrounded by a 0.318 cm thick water region. The gaps in the fuel element are assumed to be filled with helium at a pressure of one atmosphere.

Transient Results

The transient calculations were obtained for a pulse energy yield of 300 MW-sec or a single fuel element energy deposition of 1.67 MW-sec. The heat transfer code CINDA[6] was used to obtain these results for a pulse width of 4.5 msec. The radial energy deposition profile was calculated for an inner annulus U-235 loading of 500 mg/cc and an outer annulus U-235 loading of 330 mg/cc. The axial deposition profile varied according to a truncated cosine.

The effect of the thermal emissivity on the clad temperature is given in Fig. 4. The clad temperature as a function of time for emissivities of 0.8 and 1.0 is shown and the results are fairly insensitive to emissivity. For $\varepsilon = 0.8$ the clad temperature reaches a maximum value of 120° C and for $\varepsilon = 1.0$ the peak clad temperature is 126° C.

One fuel element condition of interest from a safety standpoint occurs when the outer fuel annulus comes in contact with the graphite sleeve and the sleeve makes contact with the stainless steel clad. This configuration removes the gaps between the fuel and clad and represents the maximum heat transfer condition for the fuel element. The results of calculations which simulate this condition are given in Figs. 5 and 6. The temperature of the surface of the outer fuel annulus is shown in Fig. 5. The effectiveness of the gaps in retarding heat transfer is clearly shown; when the fuel, sleeve, and clad are assumed in contact, the fuel temperature decrease is very rapid. In contrast to these results, the stainless steel clad temperature is shown in Fig. 6. With the fuel, sleeve, and clad in contact, the clad reaches a temperature slightly in excess of 270° C, which is well below the clad melting point. When the various gaps are included in the calculations, the clad temperature reaches 120° C.

Another calculation determined the effect of removing the graphite sleeve and the results are shown in Figs. 7 and 8. Without the sleeve the heat transfer is considerably reduced and the rate of temperature decrease of the outer fuel annulus is considerably reduced. The effect of the graphite sleeve on the clad temperature is shown in Fig. 8. With the sleeve the clad reaches 120° C and without the sleeve the clad reaches about 112° C.

Another configuration of interest to the safety of the fuel element occurs when the outer fuel annulus is in contact with the graphite sleeve. These results are given in Figs. 9 and 10. The graphite sleeve temperature as a function of time is shown in Fig. 9, and with the fuel touching the sleeve the graphite temperature is considerably larger. However, the clad temperature is only about 10 percent higher with the fuel touching the sleeve as shown in Fig. 10.

The worst case fuel element heat transfer would occur if the water region around the clad became a void immediately prior to a pulse. This condition was examined by removing the water region and assuming that the clad surface was an

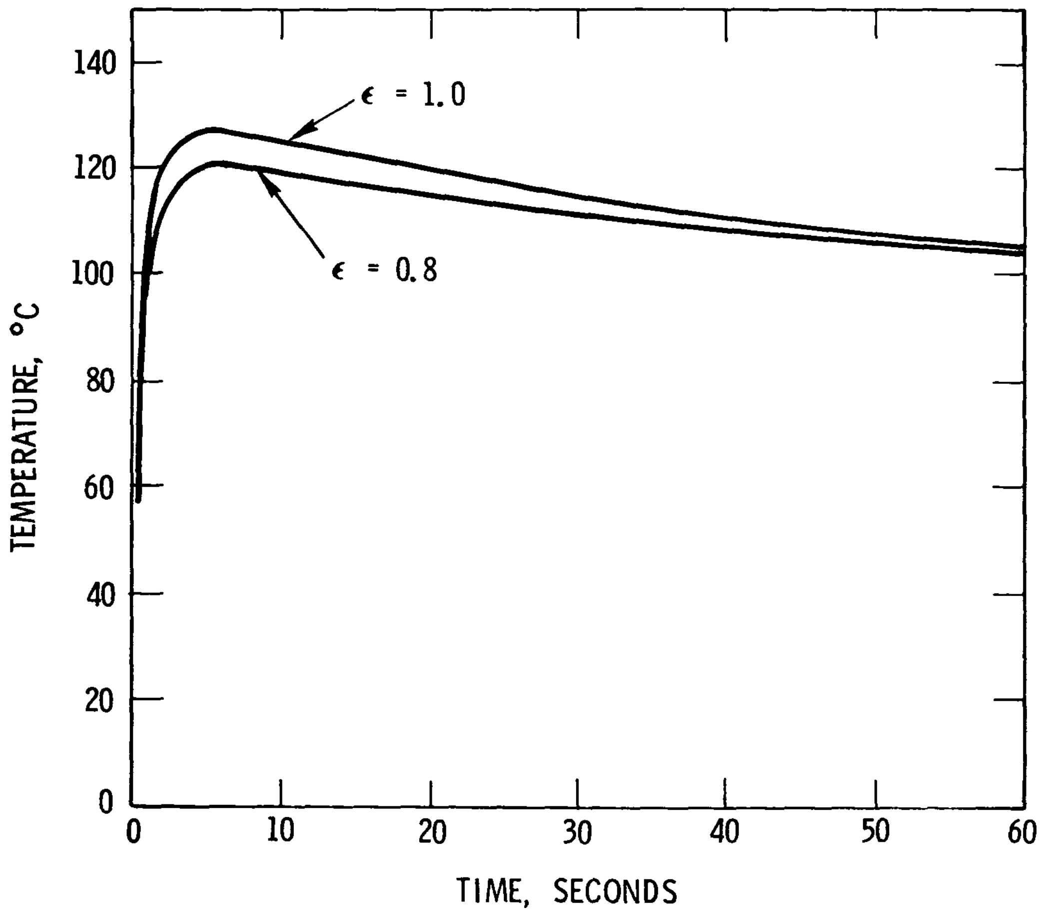

Figure 4. Effect of Emissivity on Clad Temperature

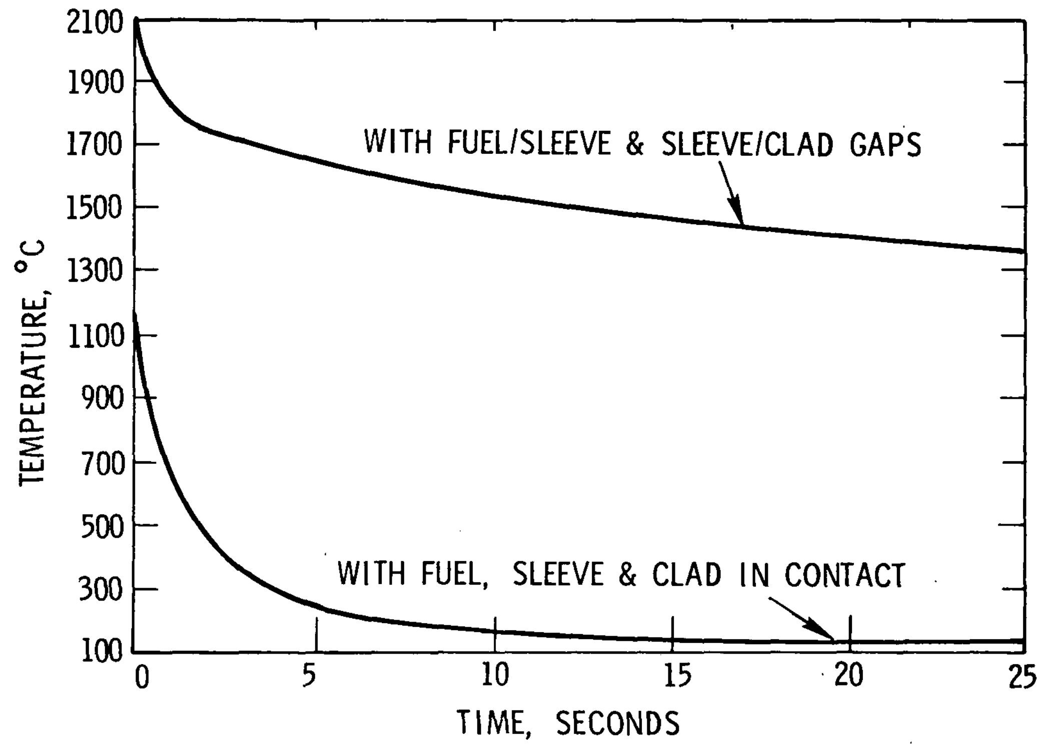

Figure 5. Outer (UC-ZrC)-C Annulus Surface Temperature

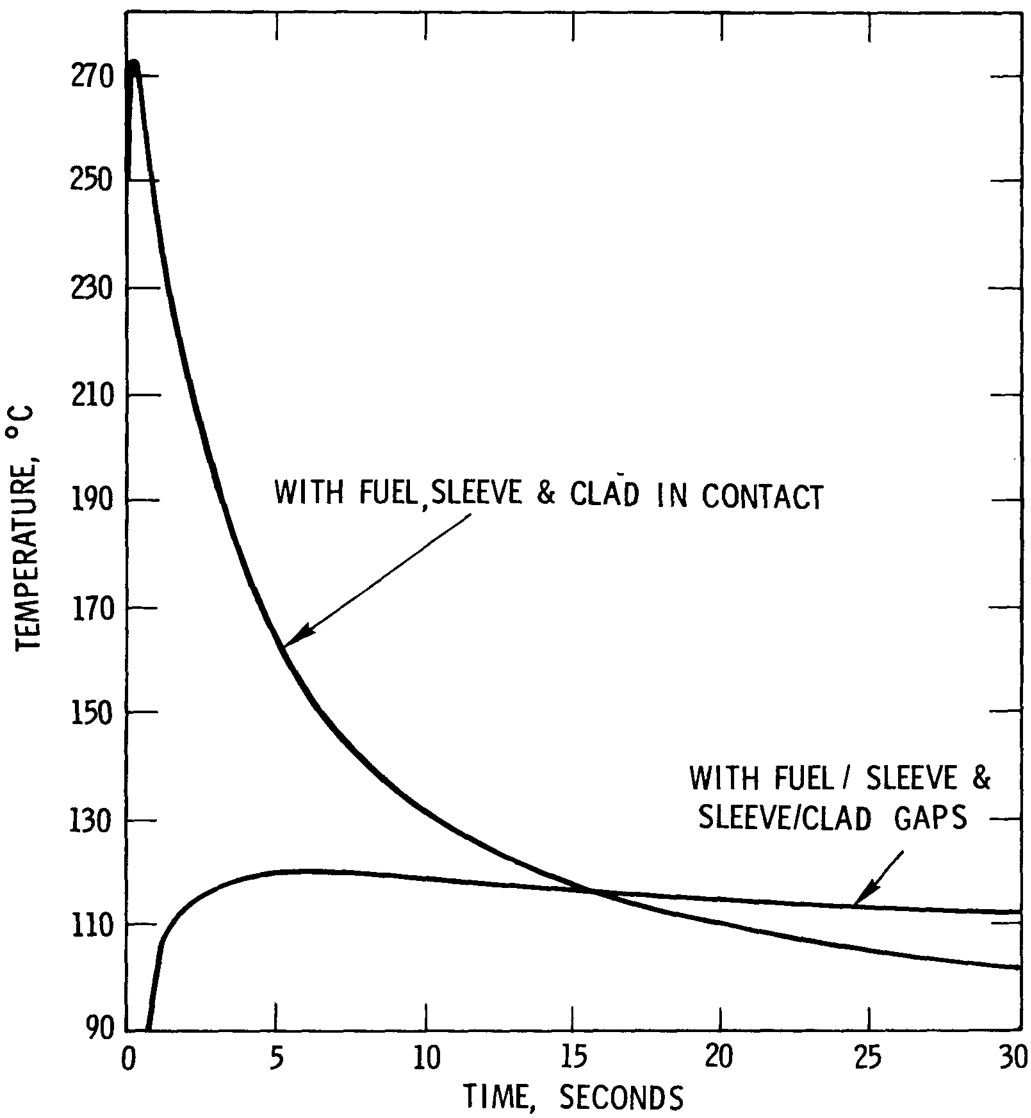

Figure 6. Stainless Steel Clad Temperature

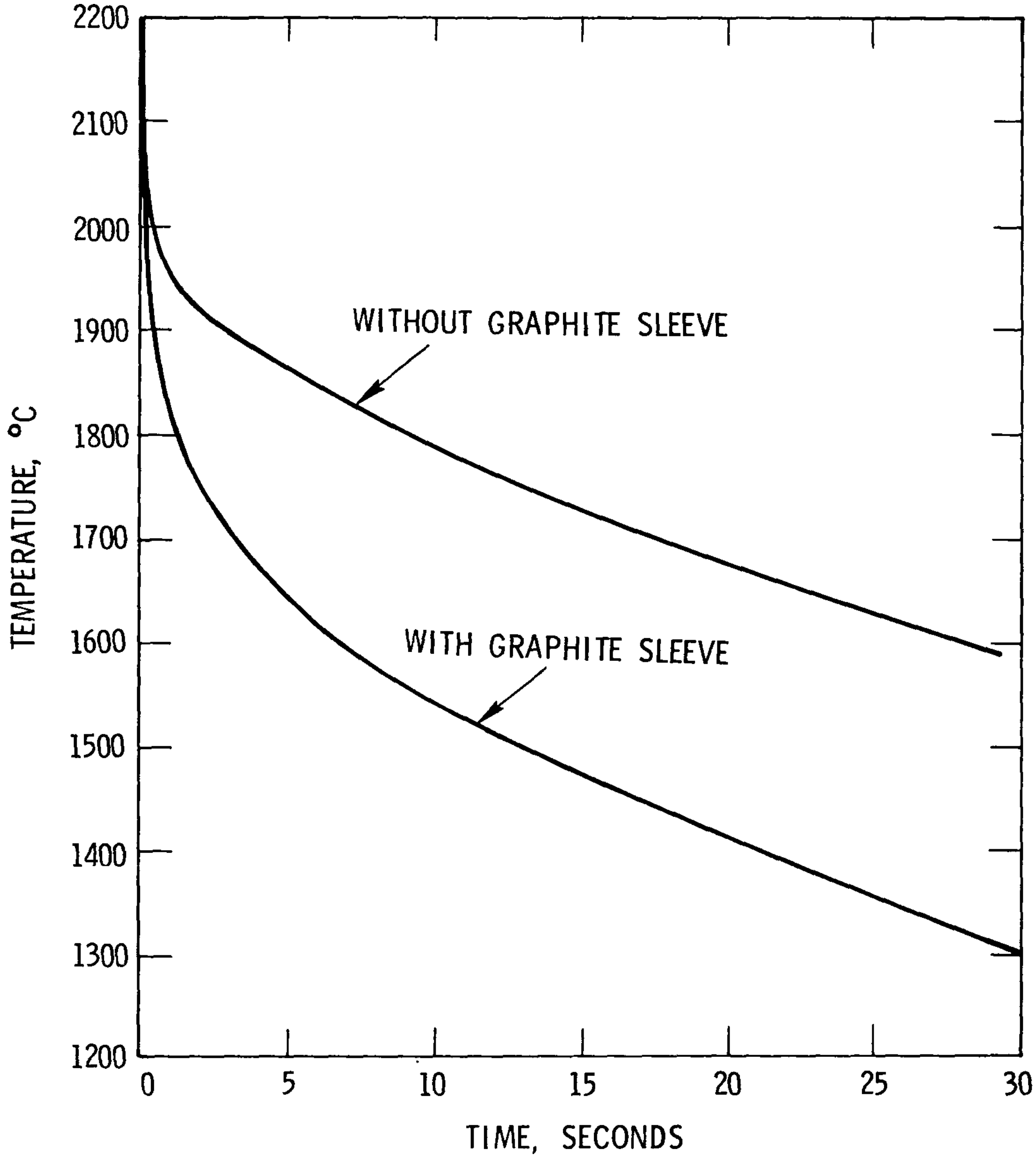

Figure 7. Outer (UC-ZrC)-C Annulus Temperature

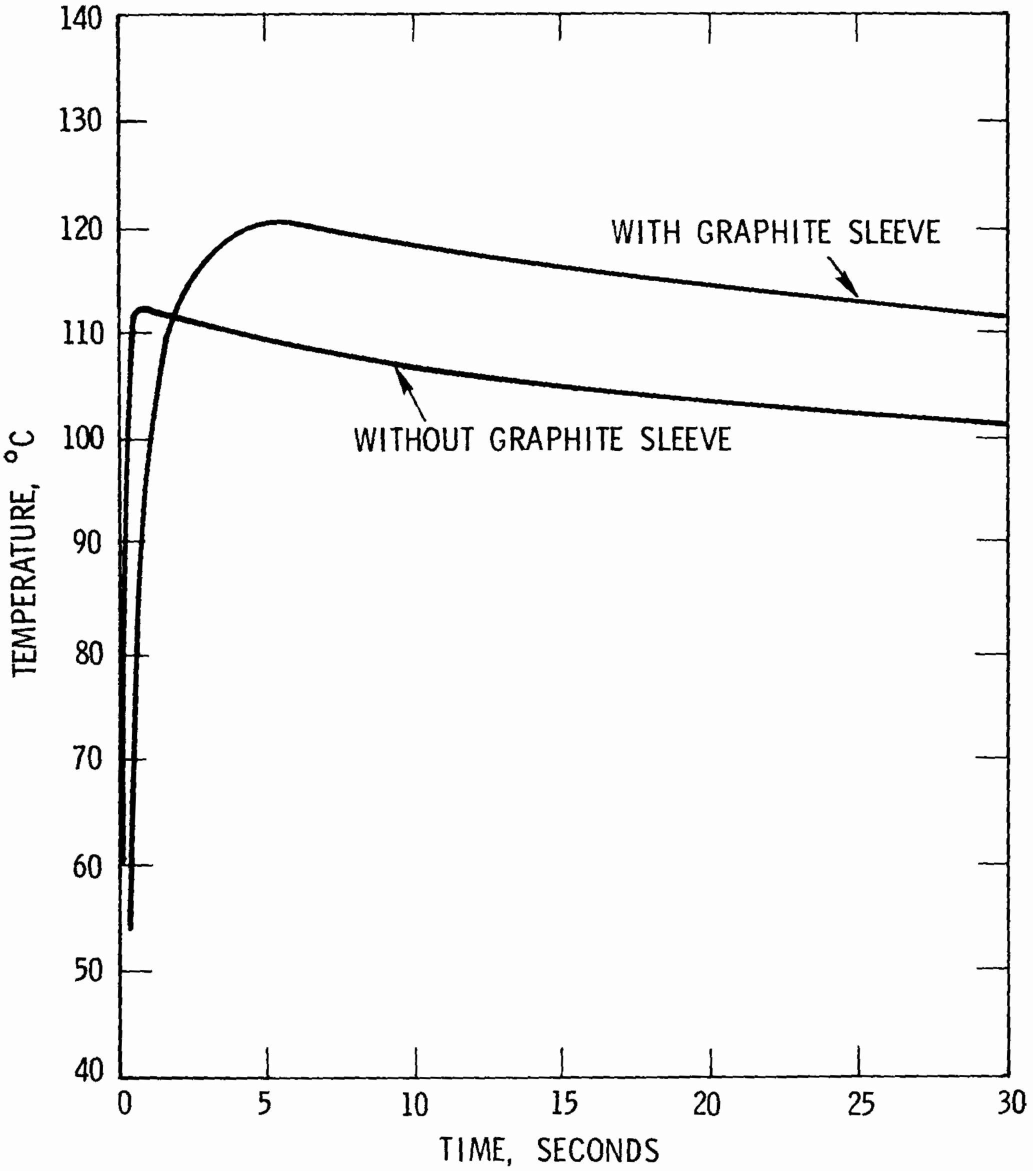

Figure 8. Stainless Steel Clad Temperature

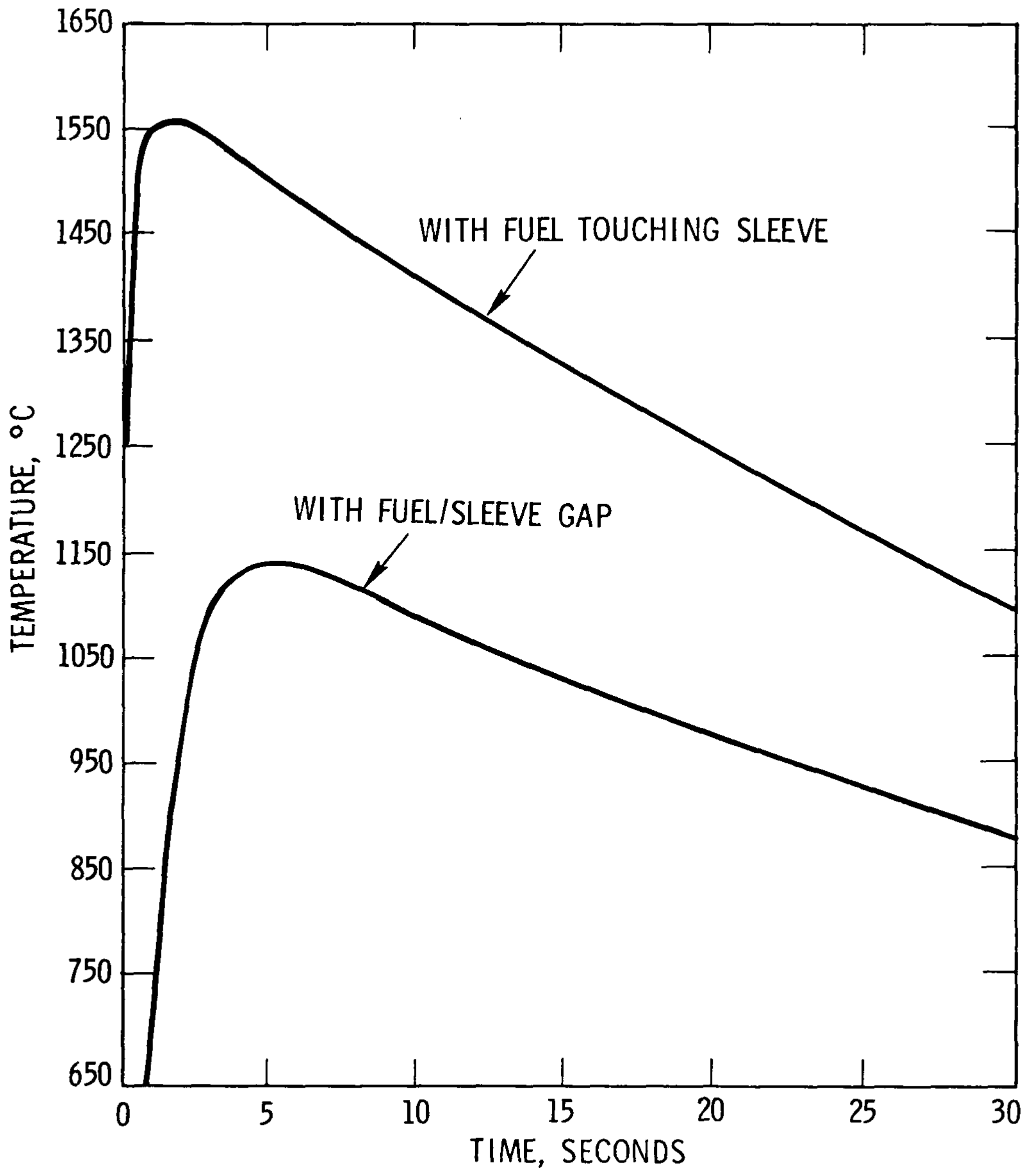

Figure 9. Graphite Sleeve Temperature

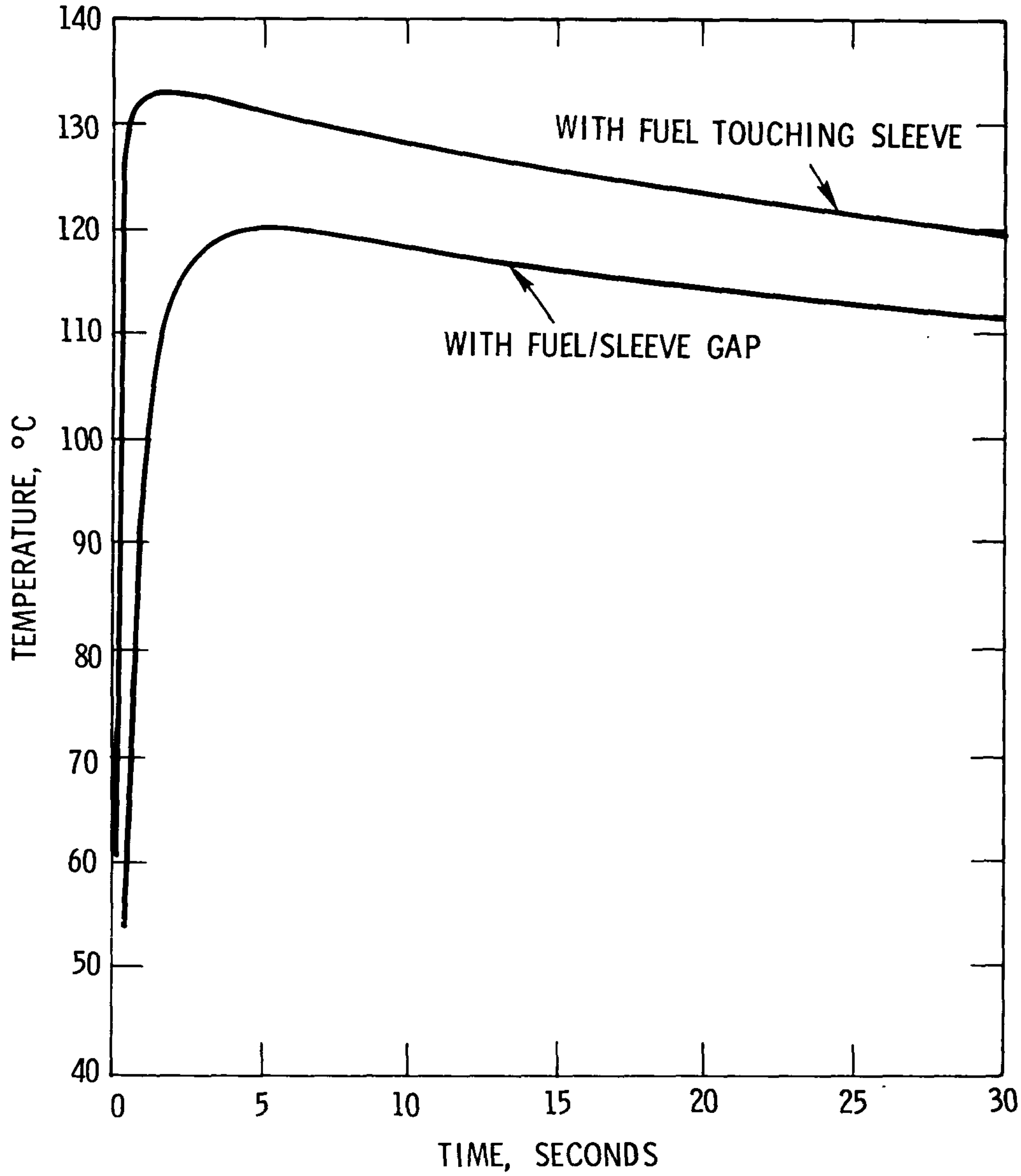

Figure 10. Stainless Steel Clad Temperature

insulated boundary. The results of these calculations are given in Fig. 11; the temperature of the outer fuel surface, the graphite sleeve and the clad are shown. The important aspect of these calculations is that the clad temperature reaches its melting point in 20 seconds. These results represent an upper limit for the dual-annulus fuel element heat transfer calculations. The importance of the water in preserving the fuel element integrity is clearly illustrated, since with the water included in the calculations the clad reaches only 120° C.

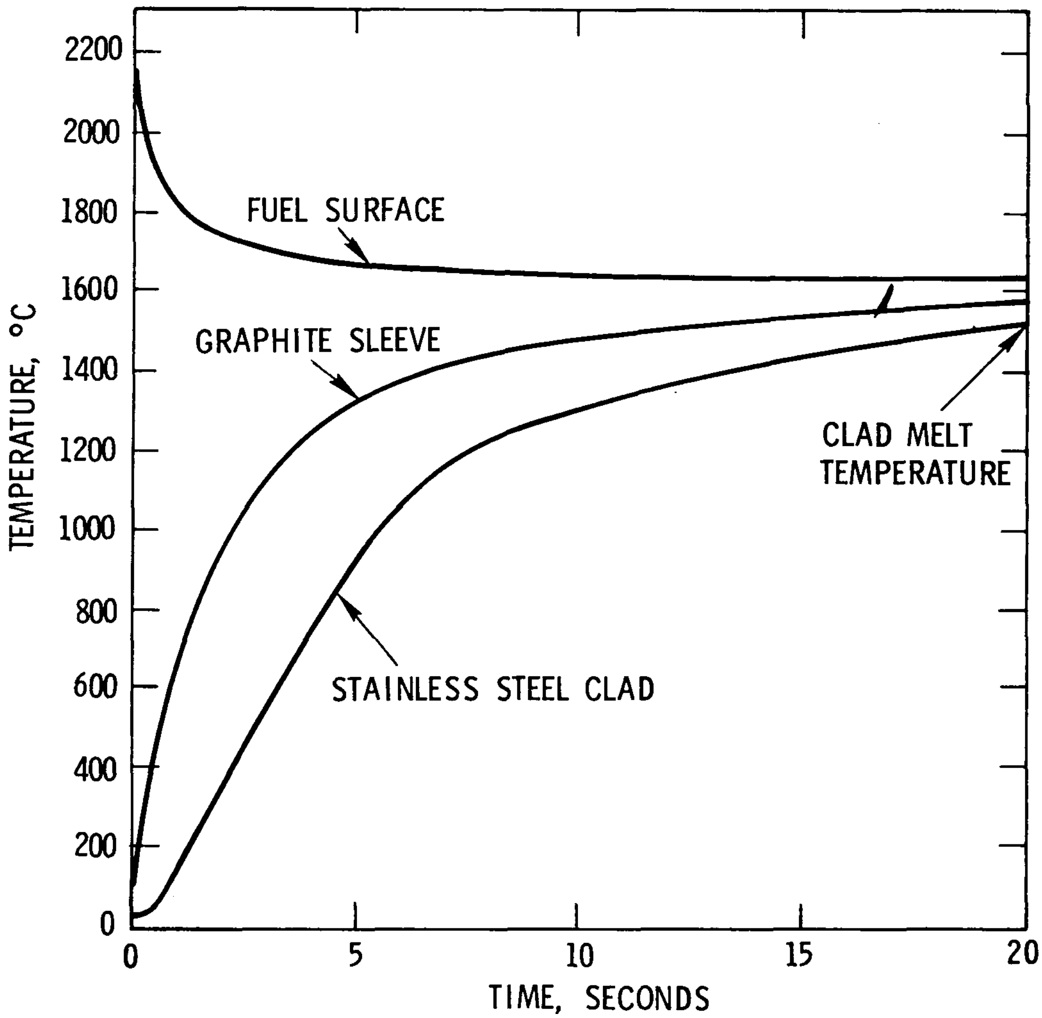

Figure 11. Temperatures in (UC-ZrC)-C Fuel Element with Water Removed

CHAPTER VI

TASK 6. PRIMARY FUEL MATERIAL STUDIES

P. S. Pickard, 5422; D. J. Sasmor, 5422

Introduction

The in-pile testing of the UO_2-BeO (15 weight percent UO_2) fuel candidate continued during this quarter. The initial tests, reported in the previous quarterly report, SAND-75-0630,[4] utilized single, 1/4-inch thick dual annuli. In subsequent tests the length of the fuel column has been increased by stacking 1/8-, 1/4-, and 1/2-inch dual annuli; an example of one fuel stack tested is shown in Fig. 12. In addition to the increase in fuel height, both the cores and sleeves (dual annuli) were multiple segmented to provide information on segment size on overall pulse test survival. The maximum temperature calculated for the outer annulus (sleeve) ranged from 494° to 1557° C. These temperatures are adiabatic temperatures based on the fission product inventory of individual samples.

In-Pile Experiments

A tabular summary of the tests performed to date is given in Table I. These tests involved 1/8-, 1/4-, and 1/2-inch high samples with segments ranging from 355 degrees (single slotted annuli) to 45 degrees. The 1/8-inch high dual annuli samples were used primarily as fission product inventory monitors and were sectioned and counted after the test. These samples survived all pulse tests in which they were used. The 1/2-inch high samples survived pulse tests up to maximum temperatures of approximately 1000° C but fractured consistently in more severe tests. All fuel tests utilized a fueled UC-ZrC-C annulus as a lower standoff. For the tests resulting in more than 1000° C in the UO_2-BeO samples, the UC-ZrC-C sleeve is driven to temperatures generally exceeding the BeO phase transition of 2050° C. It is not known how severely the 1/2-inch high UO_2-BeO samples are affected by contact with the hotter carbide sleeve, but it is assumed that the above test conditions have resulted in earlier fracture in the 1/2-inch samples than would otherwise be observed. The next series of tests will not utilize the UC-ZrC-C sleeve in an attempt to eliminate this factor from test interpretation.

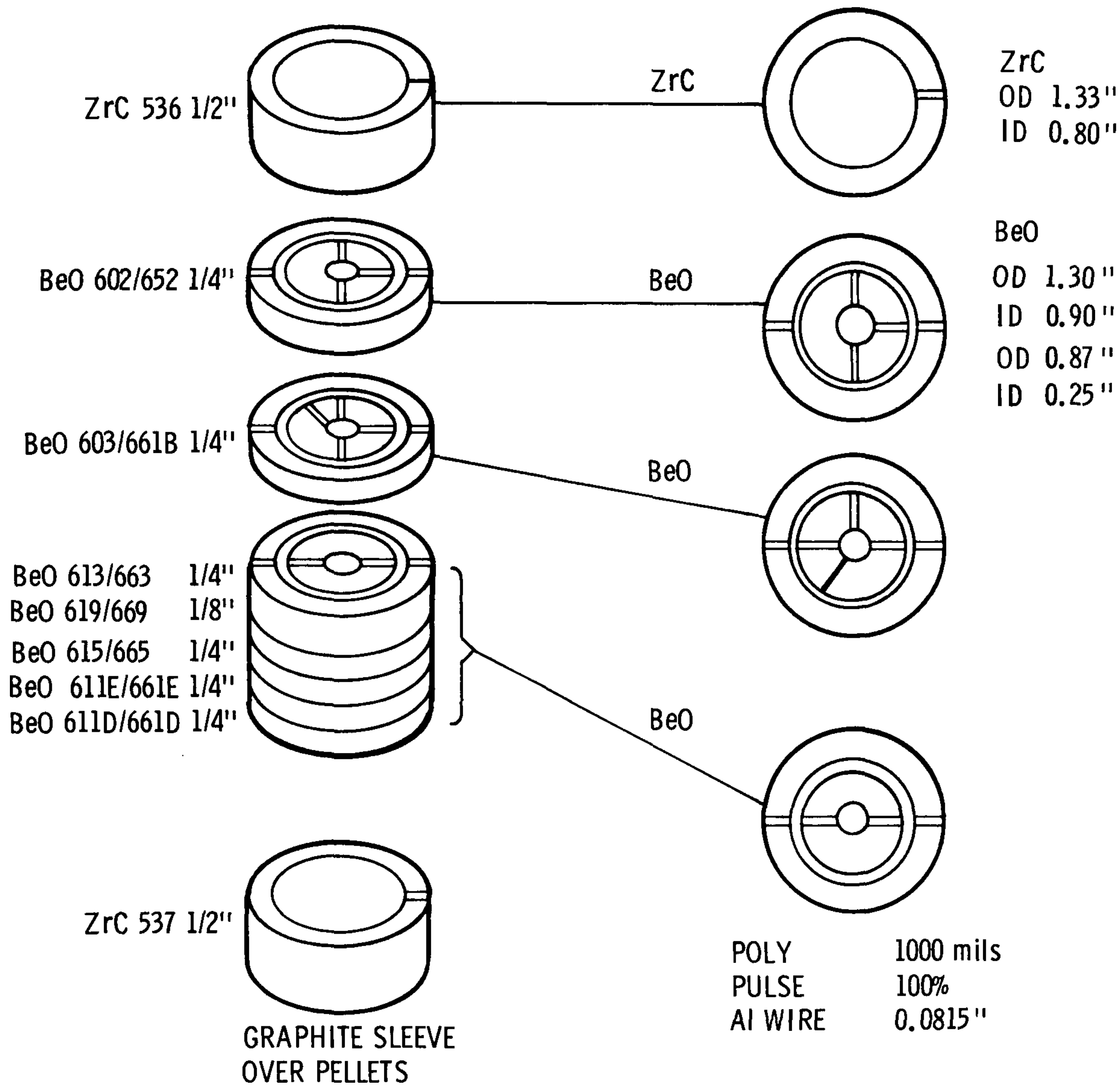

Figure 12. Test Fuel Stack Configuration for UO_2-BeO Pulse Tests

TABLE I

$BeO-UO_2$ Fuel Test Results

% of Max. Pulse	Polyethylene Moderator (Thick./inch)	$BeO-UO_2$ Fuel Column Length (Total inches)	Height (Inches) 1/2	1/4	1/8	Outer Annulus (Sleeve) Temperatures Average	Peak
75	0.00	1/4		1		435	496
50	0.5	1/4		1		545	620
50	0.5	1-1/2	2	2		545	620
75	0.5	1/4		1		762	868
75	0.5	1-1/2	2	2		762	868
100	0.5	1/4		1		967	1101
100	0.5	1-1/2	2	2		967	1101
25	0.75	1-1/8		4	1	363	447
75	0.75	1/4		1		793	903
75	0.75	1-1/2	2	2		832	948
75	0.75	1-1/2	1	4		906	1112
100	0.75	1-3/8	1	3	1	1149	1411
75	1.00	1-1/2	2	2		1005	1145
25	1.00	1-1/8		4		370	494
75	1.00	1-1/2	2	2		923	1228
100	1.00	1-5/8		6	1	1170	1557

The majority of tests to date have been performed on 1/4-inch high dual annuli samples. A summary of the history of each 1/4-inch outer annuli (sleeve) is presented in Table II. The sleeves experience the most severe stress and temperature conditions, and survival or failure criteria apply primarily to the sleeves. The cores show only infrequent failures, generally attributed to material or sample defects and the core test history will not be reproduced here.

The fission energy deposition profiles for the 3/4- and 1-inch polyethylene moderated tests are shown in Figs. 13 and 14. The estimated temperature drops across the sleeve were determined from such profiles and the calculated maximum temperatures. The data in Table II are abstracted from Table III, which shows only survival or fracture for each segment tested. Preliminary interpretation of these results suggests that survival for single pulse tests in large segments is limited to maximum temperatures of 1100° to 1200° C, while somewhat smaller segments (180 degrees) are suitable at somewhat higher levels. Additional data are being obtained to allow more definitive interpretation.

The UO_2-BeO samples tested have displayed a fairly wide band of conditions under which fracture will occur. Fractures have been observed under conditions which are considerably less severe than conditions under which similar samples have consistently survived. The cause of these premature failures is generally considered to be sample or material defects. Microscopic examination has indicated most of these premature failures are low-energy fractures which often originate at surfaces where tensile stresses are not calculated to be large. Surface flaws are assumed to be the origin of the crack and further work is being performed to verify these assumptions and to attempt to eliminate the cause.

The fracture surfaces (opposing surfaces 661A-1, 661A) shown in Fig. 15 are interpreted as high-energy fractures. This fracture occurred in a single slotted sleeve at a temperature of ~ 1230° C and probably approaches the material limit for the single slotted annulus. Typical low-energy fractures with smooth surfaces are shown in Fig. 16 (604 and 611B). These are from cores and occurred at 890° and 970° C, respectively. These may be due to large (~ 40 μ) BeO grains or imperfections in the hot pressing. The actual point of initiation on the flaw has not been uniquely identified in these early tests. Improvements in materials (i.e., smaller particle size (BeO)) and changes in pressing parameters may provide improvement in sample consistency.

The required operational temperature for the beryllia-based fuel in pulse mode is 1000° to 1200° C and requires about 7 to 8 w/o UO_2. Moderated tests in the ACPR at 1000° to 1200° C represent an overtest of about 50 to 75 percent over the

TABLE II

Sleeve Histories

(1/4" High Samples)

Sample Number	Moderator Thickness (in)	% Max Pulse	Temperature			Segment Size (Number) (°)	Sample Condition
			Ave	ΔT*	Max		
651	0	75	435	-	496	360	No change
	0.5	100	967	400	1101	360	No change
652	0.5	50	545	230	620	360	No change
	0.5	75	762	320	868	180(2)	No change
	0.5	100	967	400	1101	180(2)	No change
	0.75	100	1180	560	1414	180(2)	No change
	.75	75	906	440	1112	180(2)	Single Crack ≃ 90° in one sample No change in other
	1.0	100	1170	650	1557	180(2)	1 sample cracked in preparation 2 large cracks, several small cracks in other sample
653	0.5	75	762	320	868	90(2),135,45	No change
	0.5	75	762	320	868	90(2),135,45	No change
	0.5	100	967	400	1101	90(2),135,45	No change
	0.75	100	1150	560	1[illegible]11	90(2),135,45	1 90° sample broke at ≃45°
654	0.75	.75	832	380	943	360	No change
	0.75	.25	363	180	447	360	No change
661A	0.5	50	545	230	620	360	No change
	0.75	75	832	380	948	360	No change
	1.0	75	923	510	1228	360	Broke ~180° from slot
661B	0.5	50	545	230	620	180(2)	No change
	0.75	75	832	380	948	180(2)	No change
	1.0	75	923	510	1228	180(2)	No change
	1.0	100	1170	650	1557	180(2)	1 sample cracked ≃ 75
661D	0.75	25	363	180	447	180(2)	No change
	1.0	100	1170	650	1559	180(2)	No change
661E	0.75	25	363	180	447	180(2)	No change
	1.0	100	1170	650	1557	180(2)	1 sample cracked ≃ 80°
663	1.0	25	370	200	490	360	No change
	1.0	100	1170	650	1557	180(2)	1 sample cracked ≃ 30°
664	1.0	25	370	200	490	180(2)	No change
665	1.0	25	370	200	490	180(2)	No change
	1.0	100	1170	650	1559	180(2)	1 sample cracked ≃ 80°
666	1.0	25	370	200	490	360	No change

*Estimated adiabatic temperature drop across sleeve

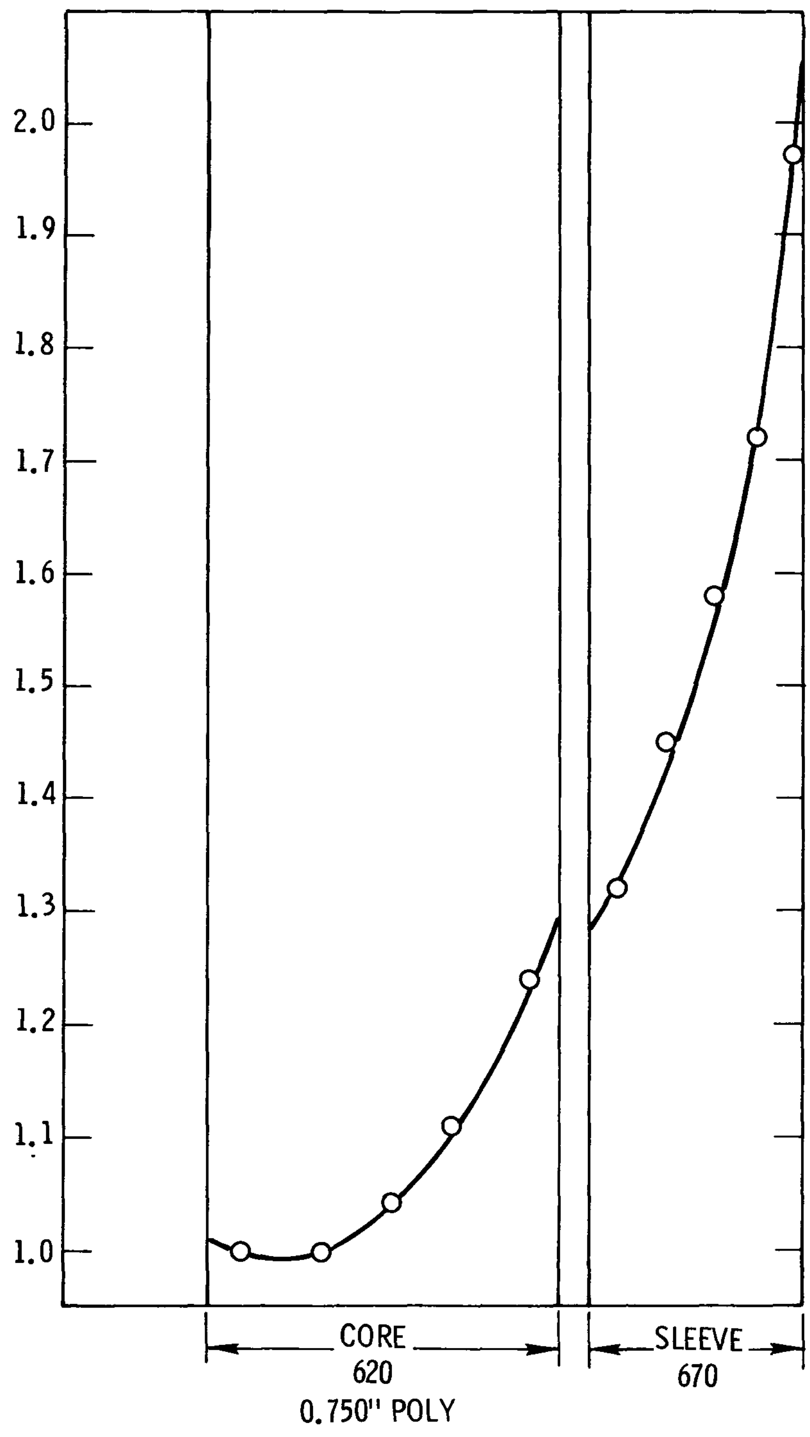

Figure 13. Fission Energy Deposition Profile in 15 w/o UO_2-BeO Pellets for 0.75 Inch Polyethylene Moderator Tests

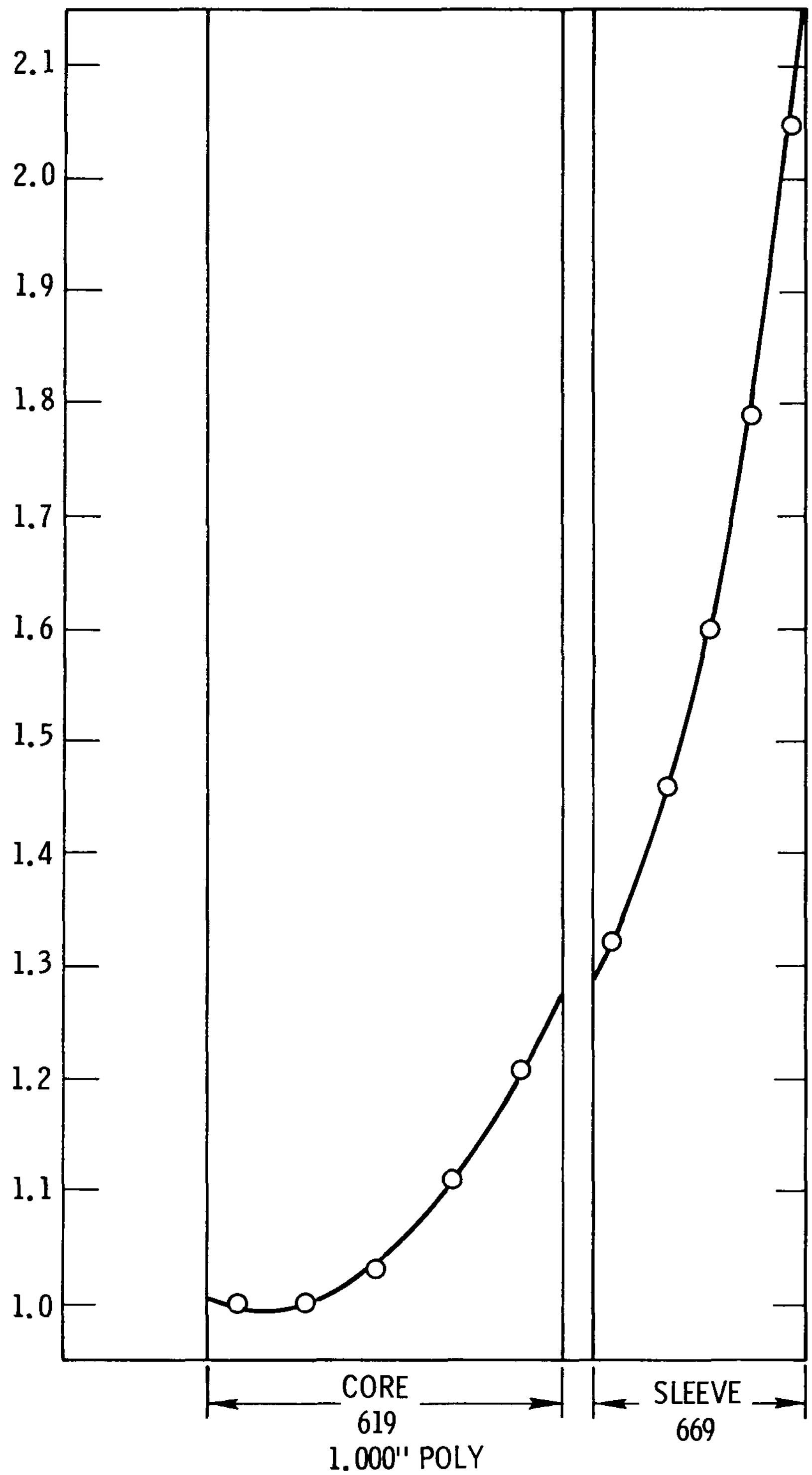

Figure 14. Fission Energy Deposition Profile in 15 w/o UO_2-BeO Pellets for 1 Inch Polyethylene Moderator Tests

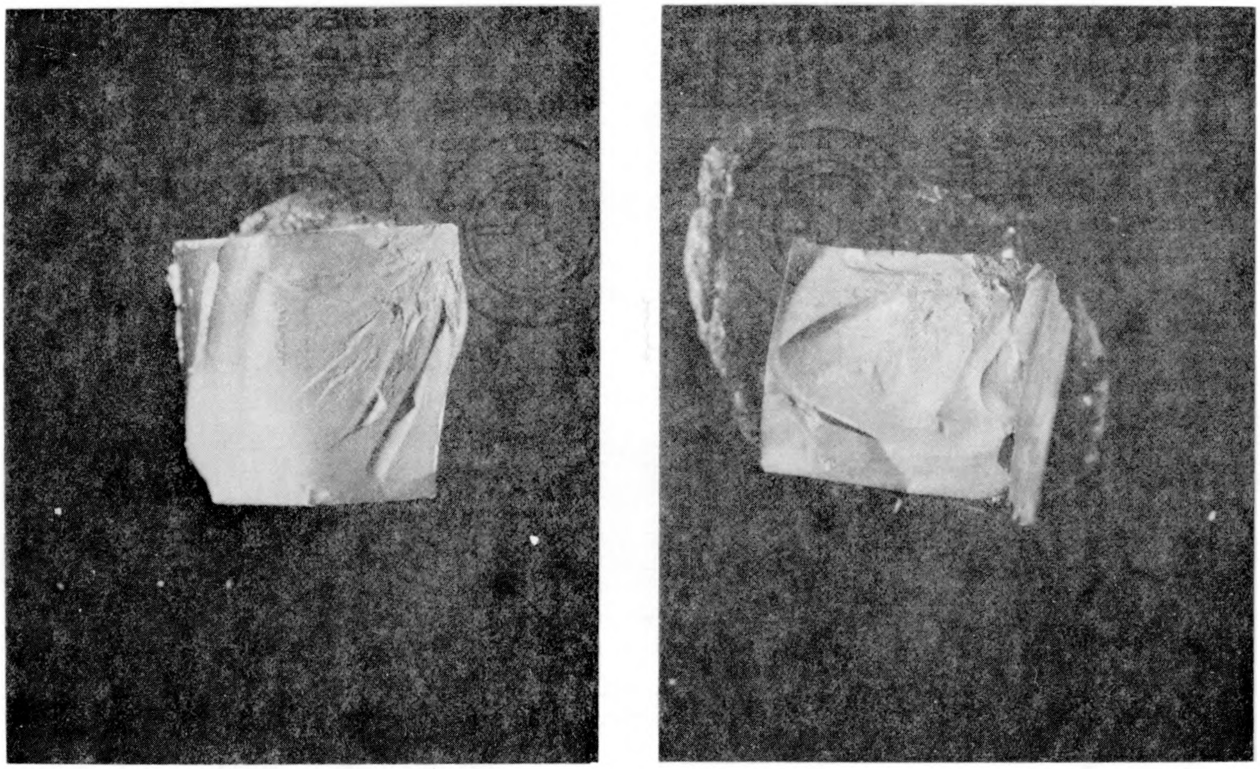

661A-1 661A

Figure 15. Fractured Surfaces for 15 w/o UO_2-BeO Pellets (high energy)

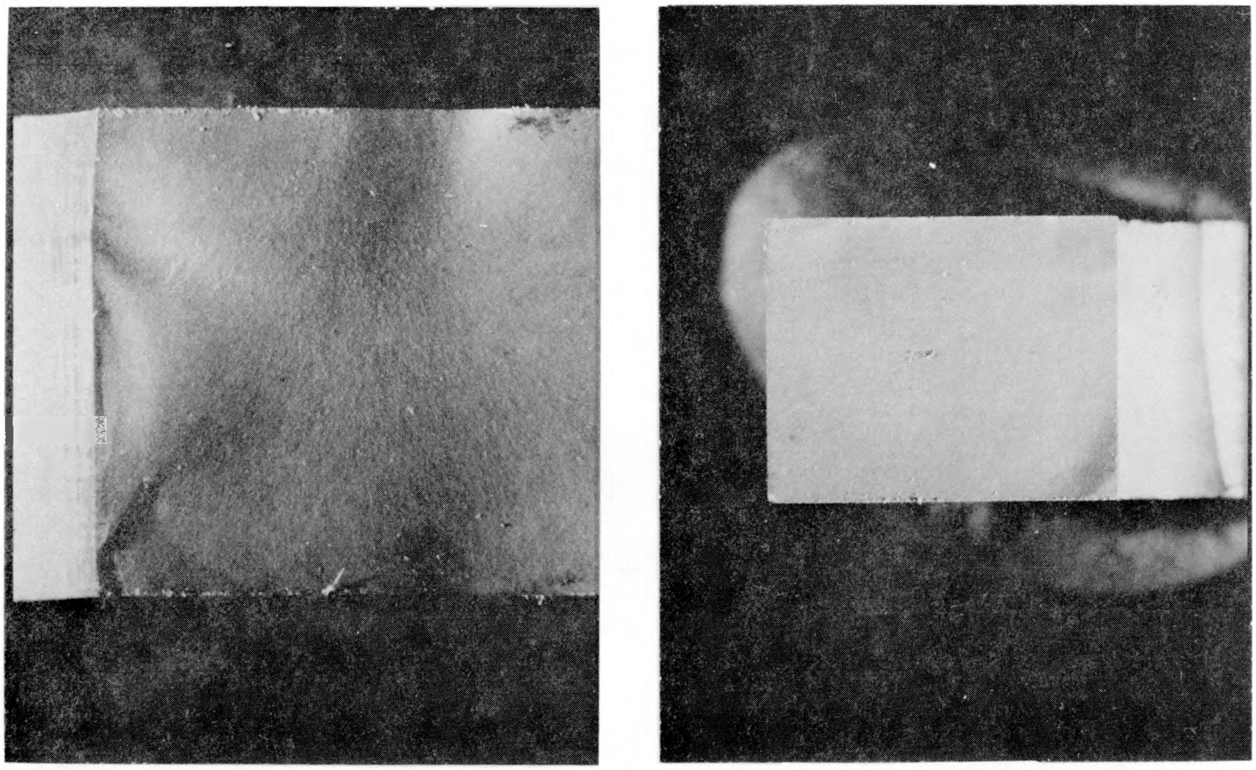

604 611B

Figure 16. Fractured Surfaces for 15 w/o UO_2-BeO Pellets (low energy)

estimated stress in the pellet in the upgrade core. The next series of experiments on the BeO-UO_2 fuel involves multiple-pulse tests on the 15 w/o UO_2 hot pressed material to assess the behavior of the fuel under repeated thermal shock. These repetitive tests will evaluate both the pellet fracture resistance and the consequences of pulse operation with fractured pellets in the fuel column. These results should provide adequate information for the evaluation of the BeO-UO_2 fuel candidate.

CHAPTER VII

TASK 7. SECONDARY FUEL MATERIAL STUDIES

R. H. Marion, 5847; C. H. Karnes, 5847; R. A. Sallach, 5831

Introduction

The secondary fuel material studies during this quarter concentrated on hot-pressed and extruded material. Samples from each fabrication process were tested in the ACPR to 2000° C or greater without fracture.

Hot-Pressed (U, Zr)C-Graphite

Fuel samples have been prepared at LASL by hot pressing a mixture containing 35 vol % (U,Zr)C (average particle size ≅ 3.5 μm) with the balance made up of -325 mesh (< 45 μm) KX-88 graphite flour and voids. The hot pressing was performed at approximately 2650° C and pressures up to 24.8 MPa (3600 psi). High-density (open porosity ≅ 11%) and low-density (open porosity 18%) solid pressings 33 mm in diameter by 76.2 mm long were prepared by varying the pressure during the hot pressing. Each pressing was cut into a number of fuel pellets 3.18 mm, 12.7 mm, and 25.4 mm long. The bulk density of individual pellets cut from a particular pressing varied by 6%. All the pellets had a uranium content of 360 - 380 mg/cc of 90.7 percent enriched uranium.

The microstructure of this material is significantly different from the extruded dual annulus material discussed in the last quarterly report. Almost all the (U,Zr)C agglomerates are less than 40 μm in size and they are all well-separated by graphite particles and voids. There is no interlocking network of (U,Zr)C similar to that observed in the extruded material. The low-density and the high-density, hot-pressed materials have similar (U,Zr)C distribution but they differ in the degree of sintering of the composite. The high-density material has better bonding within the composite and the voids are uniformly distributed with a size of less than 10 μm. The low density materials have most of the porosity stretched out along the grain boundaries between the graphite and carbide particles and the composite was not sintered as well.

Solid pellets up to 25.4 mm long of both the high-density and low-density material were tested in the ACPR. The severity of the test condition was increased until failure was obtained in both materials. Failure was not obtained in either the 3.18 mm or the 12.7 mm long pellets.

The 25.4 mm long low-density pellets failed at an average energy deposition of 220 - 240 cal/g with a peak/minimum in the pellet equal to 2.17 and a peak/average equal to 1.47. This corresponds to a peak temperature in the pellet of about 1600° C.

The 25.4 mm long high-density pellets could not be failed at an average energy deposition of 306 cal/g with a peak/minimum equal to 2.17. This corresponds to a peak temperature equal to 2000° C. However, when the peak/minimum energy deposition was increased to 2.22 by increasing the polyethylene moderator thickness from 19.05 to 25.4 mm, the 25.4 mm long pellet failed between 245 cal/g and 275 cal/g. (Approximately 1700 - 1900° C).

Extruded Dual Annulus (U,Zr)C-Graphite Fuel

Further material characterization has been performed on the extruded dual annulus materials described in the preceding quarterly report. Scanning electron microscopy has been performed on the fracture surfaces of two outer annuli which were pulsed in the ACPR to maximum temperatures of 2135° C and 1950° C. There are a number of regions where the (U,Zr)C particles have become rounded and grown larger (sintered). The microstructure is quite different than that observed in unirradiated specimens, and it has been tentatively concluded that the carbide phase may be melting in the composite. This implies that thermal equilibrium is not present between the graphite and carbide phases because of the large carbide particles.

Preliminary results on the distribution of uranium in the (U,Zr)C particles have been obtained on an electron beam microprobe. For particle sizes in excess of 40 μm, the uranium loading is not uniform throughout the particle because the diffusion time during processing is insufficient to allow complete penetration.

Additional Fuel Development

A new extruded fuel is currently being produced at LASL which incorporates many of the process changes suggested by the results of earlier tests and analyses.

The fuel material is being fabricated in the slotted, dual annulus geometry in order to eliminate the need for adapting the process to the design geometry at a later date. In order to reduce the bulk (composite) thermal expansion coefficient, the carbide content is being reduced to 30 and 20 vol % for the inner and outer annuli, respectively, and a low thermal expansion graphite flour (9553) is being utilized. The open porosity is being retained at approximately 20 percent by the use of tapioca as a pore former. The carbide is included as (U,Zr)C solid solution particles whose average size is approximately 3.5 μm. This material is scheduled to be delivered in early January along with tensile specimens for independent mechanical property measurements.

Several new processes incorporating both hot pressing and extrusion have been identified and are currently being initiated at LASL. They are described below.

Hot Pressing

(a) Material is being made which is identical to the high-density, hot-pressed material previously evaluated except that -325 mesh low thermal expansion 9553 graphite flour is being used instead of KX-88 flour. The carbide content is to be 30 vol %.

(b) In order to reduce the graphite particle size further to get a better distribution of carbide, graphite, and porosity, 9553 graphite flour will be used which has been milled in a fluid energy mill and separated to retain all particles less than 10 μm. The process is otherwise identical to Part (a) above.

(c) An additional batch of hot-pressed material is to be made identical to Part (a) above, except that approximately 15 vol % low thermal expansion graphite fibers are to be included.

Extrusion

(a) A fuel having no zirconium, just UC_2 and graphite, is to be made utilizing -325 mesh 9553 graphite and tapioca pore former to create just enough porosity to allow the extrusions to survive the heat treat processes. The final heat treatment will be done at 2350° C in order to prevent melting of the UC_2. The very low carbide content (~ 5%) should produce a significantly higher enthalpy at high temperatures and a lower thermal expansion.

(b) An additional lot of material following the same process as Part (b), except incorporating 15 vol % carbide, is to be made. The UC_2/graphite fuel will be subject to hydrolysis and the 15 vol % carbide is sufficient for stabilization.

(c) A feasibility study is being initiated on a material made by loading uranium atoms onto a monomer, curing and carbonizing the resin, then grinding it into a fine flour to be incorporated into LASL's extrusion process. The flour can be made at ORNL. It will contain atomic ratios of C/U = 15 and S/U = 1. It is similar to the HTGR fuel which ORNL is currently making, but, when ground and extruded, will result in a fuel having the fissile material uniformly dispersed in the particle rather than in the grain boundaries, as exists in current carbide/graphite fuels.

Materials Compatibility

A review of the extensive literature on graphite/stainless steel interactions has been made. Carburization, the isothermal dissolution of carbon and/or the formation of carbide, becomes noticeable at 600° C and proceeds rapidly at 850° C. Graphitization is a closely related process in which carbon dissolved at higher temperatures precipitates as graphite on cooling. A combination of these processes may occur when the metal is in a thermal gradient.

Preliminary heat transfer calculations for pulsed operation of the reactor indicate that temperatures greater than 270° C may be reached at the inner stainless steel surface, if the graphite sleeve is in good thermal contact with both the fuel and the stainless steel clad. Thus no clear-cut prediction of damage or the lack of it is possible. Accordingly, experiments have been conceived whereby the interface reaction between graphite and stainless steel (in a thermal gradient) can be studied simulating either pulsed or steady-state operation of the reactor.

For the pulsed mode, experiments will be based on laser irradiation techniques. Experiments simulating steady-state operation will be performed with a resistive heating system known in materials testing circles as the "Gleeble." Specimen preparation is now in progress.

CHAPTER VIII

TASK 8. DRIVER CORE FUEL ELEMENT

J. A. Reuscher, 5421

Introduction

The outer region of the upgraded ACPR will consist of uranium-zirconium hydride fuel elements similar to the elements in the present ACPR core. This task involves the in-pile testing and design of the U-ZrH fuel element.

In-Pile Tests

The test specimens of uranium-zirconium hydride for the in-pile tests have been ordered from General Atomic, San Diego, and delivery is expected in April, 1976. The hydrogen-to-zirconium ratio in the specimens will vary about 1.5 and the uranium will be fully enriched. The design of the pressure container to be used in the reactor tests was begun. This container is to be made from a short length of dimpled clad and will be used for the element section tests with the high heat capacity fuels.

CHAPTER IX

TASK 9. DIAGNOSTIC SYSTEM

Activities on this task for this reporting period are described in Experimental Fast Reactor Safety Research Program - Quarterly Report, July-September 1975, SAND75-0567, Reactor Research and Development Department, Sandia Laboratories, Albuquerque, New Mexico, November 1975.

References

1. Experimental Fast Reactor Safety Research Program - (Combined) Quarterly Report, July-December 1974, SAND75-0068, Simulation Sciences Research Department, Sandia Laboratories, Albuquerque, New Mexico, February 1975.

2. Experimental Fast Reactor Safety Research Program - Quarterly Report, January-March 1975, SAND75-0225, Simulation Sciences Research Department, Sandia Laboratories, Albuquerque, New Mexico, April 1975.

3. Experimental Fast Reactor Safety Research Program - Quarterly Report, April-June 1975, SAND75-0449, Reactor Applications Research Department, Sandia Laboratories, Albuquerque, New Mexico, August 1975.

4. Annular Core Pulse Reactor Upgrade - Quarterly Report, July-September 1975, SAND 75-0630, Reactor Research and Development Department, Sandia Laboratories, Albuquerque, New Mexico, January 1976.

5. Experimental Fast Reactor Safety Research Program - Quarterly Report, July-September 1975, SAND75-0567, Reactor Research and Development Department, Sandia Laboratories, Albuquerque, New Mexico, November 1975.

6. J. D. Gaski, Chrysler Improved Numerical Differential Analyzer for Third Generation Computers, TN-AP-67-287, Chrysler Corporation, October 20, 1967.

DISTRIBUTION:

TID-4500 - NRC-7 (259)

Division of Reactor Safety Research (2)
U.S. Nuclear Regulatory Commission
Washington, D.C. 20555
Attn: W. S. Farmer, Plant Engineering Branch
J. C. Stone, Plant Engineering Branch

Division of Reactor Safety Research (7)
Office of Nuclear Regulatory Research
U.S. Nuclear Regulatory Commission
Mail Station: G 158
Washington, D.C. 20555
Attn: M. Silberberg, Chief, Experimental Fast Reactor Safety Branch (1)
R. W. Wright, Experimental Fast Reactor Safety Branch (6)

R. G. Smith, Director (7)
Research Coordination Group
Office of Nuclear Regulatory Research
U.S. Nuclear Regulatory Commission
Mail Station: Nickelsen Lane
Washington, D.C. 20555

M. A. Bell
Reactor Safety Branch
Division of Operational Safety
USERDA
Washington, D.C. 20545

Division of Military Applications (2)
Office of Safety and Facilities
USERDA
Washington, D.C.
Attn: H. M. Busey (1)
Cdr. R. Bredderman (1)

Reactor Safety Research Coordination (4)
USERDA
Washington, D.C. 20545
Attn: R. W. Barber, Acting Director (3)
T. E. McSpadden, Project Manager (1)

W. H. Hannum
Division of Reactor Research and Development
USERDA
Washington, D.C. 20545

J. R. Roeder, Director
Operational Safety Division
USERDA/ALO
Albuquerque, New Mexico 87115

K. E. Elliott
Operational Safety Division
USERDA/ALO
Albuquerque, New Mexico 87115

DISTRIBUTION (cont)

C. B. Quinn
Special Programs Division
USERDA/ALO
Albuquerque, New Mexico 87115

M. E. Autio
Engineering and Construction Division
USERDA/ALO
Albuquerque, New Mexico 87115

Argonne National Laboratory (3)
9700 South Cass Avenue
Argonne, Illinois 60439
Attn: Robert Avery (1)
R. G. Matlock (1)
D. Rardin (1)

J. B. Holt
Inorganic Materials Division
Lawrence Livermore Laboratory
Livermore, California 94550

Los Alamos Scientific Laboratory (4)
Los Alamos, New Mexico 87544
Attn: K. V. Davidson, CMB-6 (1)
W. G. Davey, A-DO (1)
R. E. Peterson, DIR-FMO (1)
T. F. Wimett, A-5 (1)

W. E. Kastenberg
University of California
Energy and Kinetics Department
5530 Boelter Hall
Los Angeles, California 90024

Robert Seale
Department of Nuclear Engineering
University of Arizona
Tucson, Arizona

General Electric Corporation (2)
310 De Guigne Drive
Sunnyvale, California 94086
Attn: J. O. Bradfute (1)
S. Kraus (1)

R. H. Peters
TRIGA Division
General Atomic Co.
P. O. Box 81608
San Diego, California 92138

Shinzo Saito
Reactivity Accident Laboratory,
Division of Reactor Safety,
Reactor Safety Research Centre,
Japan Atomic Energy Research Institute
Tokai-Mura, Ibaraki-Ken, Japan

Electric Power Research Institute (3)
3412 Hillview Avenue
P. O. Box 10412
Palo Alto, California 94304
Attn: M. Levenson (1)
W. Loewenstein (2)

2 W. J. Howard
1000 G. A. Fowler
1100 C. D. Broyles
1126 G. L. Ogle
1130 H. E. Viney
1134 G. W. Barr
1134 J. A. Brammer
1200 W. A. Gardner
1280 T. B. Lane
1283 H. C. Hardee
1283 C. B. Sisson
1300 D. B. Shuster
3224 W. H. Myers
3241 S. N. Gaeto
3310 W. H. Kingsley
4010 C. Winter
5000 A. Narath
5100 J. K. Galt
5110 F. L. Vook
5120 G. J. Simmons
5130 G. A. Samara
5160 W. Herrmann
5200 E. H. Beckner
5200 M. J. Becktell
5230 M. Cowan, Jr.
5232 L. D. Posey
5240 G. Yonas
5400 A. W. Snyder
5410 D. J. McCloskey
5420 J. V. Walker (10)
5420A H. D. Kubiak
5421 J. A. Reuscher (10)
5421 F. M. Morris
5422 R. L. Coats
5422 P. S. Pickard
5422 D. J. Sasmor
5422 T. R. Schmidt
5423 J. E. Powell
5423 G. A. Carlson
5423 L. M. Choate
5423 L. R. Edwards
5423 J. G. Kelly
5423 W. H. Sullivan
5423 S. A. Wright
5430 R. M. Jefferson
5440 H. D. Sivinski
5700 J. H. Scott
5800 R. S. Claassen
5820 R. L. Schwoebel
5830 M. J. Davis

DISTRIBUTION (Cont)

5840	D. M. Schuster
5847	C. H. Karnes
5847	R. H. Marion
8300	B. F. Murphey
8310	R. H. Meinken
8314	G. J. Thomas
9512	W. P. Thomas
9700	R. E. Hopper
9750	R. W. Hunnicutt
9750	F. J. Tuffs
8266	E. A. Aas (2)
3141	C. A. Pepmueller (Actg) (5)
3151	W. L. Garner (3)
	For ERDA/TIC (unlimited Release)